

This item was submitted to [Loughborough's Research Repository](#) by the author.
Items in Figshare are protected by copyright, with all rights reserved, unless otherwise indicated.

Macroscopic dynamics of incoherent soliton ensembles: soliton-gas kinetics and direct numerical modelling

PLEASE CITE THE PUBLISHED VERSION

<http://dx.doi.org/10.1209/0295-5075/113/30003>

PUBLISHER

© European Physical Society

VERSION

AM (Accepted Manuscript)

PUBLISHER STATEMENT

This work is made available according to the conditions of the Creative Commons Attribution-NonCommercial-NoDerivatives 4.0 International (CC BY-NC-ND 4.0) licence. Full details of this licence are available at:
<https://creativecommons.org/licenses/by-nc-nd/4.0/>

LICENCE

CC BY-NC-ND 4.0

REPOSITORY RECORD

Carbone, F., D. Dutykh, and G.A. El. 2019. "Macroscopic Dynamics of Incoherent Soliton Ensembles: Soliton-gas Kinetics and Direct Numerical Modelling". figshare. <https://hdl.handle.net/2134/20416>.

Macroscopic dynamics of incoherent soliton ensembles: soliton-gas kinetics and direct numerical modelling

F. CARBONE¹, D. DUTYKH² AND G.A. EL³

¹ CNR-IIA, Istituto Inquinamento Atmosferico, CNR, U.O.S. di Rende, c/o: UNICAL-Polifunzionale, 87036 Rende, Italy

² LAMA, UMR 5127 CNRS, Université Savoie Mont Blanc, Campus Scientifique, 73376 Le Bourget-du-Lac, France

³ Department of Mathematical Sciences, Loughborough University, Loughborough, LE11 3TU, UK

PACS 05.45.Yv – Solitons

Abstract – We undertake a detailed comparison of the results of direct numerical simulations of the soliton gas dynamics for the Korteweg – de Vries equation with the analytical predictions inferred from the exact solutions of the relevant kinetic equation for solitons. Two model problems are considered: (i) the propagation of a ‘trial’ soliton through a one-component ‘cold’ soliton gas consisting of randomly distributed solitons of approximately the same amplitude; and (ii) the collision of two cold soliton gases of different amplitudes (the soliton gas shock tube problem) leading to the formation of an expanding incoherent dispersive shock wave. In both cases excellent agreement is observed between the analytical predictions of the soliton gas kinetics and the direct numerical simulations. Our results confirm relevance of the kinetic equation for solitons as a quantitatively accurate model for macroscopic non-equilibrium dynamics of incoherent soliton ensembles.

Introduction. – Dynamics of incoherent nonlinear dispersive waves have been the subject of very active research in nonlinear physics for several decades, most notably in the contexts of ocean wave dynamics and nonlinear optics (see *e.g.* [1–3]). Two major areas where statistical properties of random ensembles of nonlinear waves play essential role are wave turbulence and rogue wave studies (see [4, 5] and references therein). A very recent direction in the statistical theory of nonlinear dispersive waves introduced by V.E. Zakharov is *turbulence in integrable systems* [6]. It was suggested in [6] that many questions pertinent to a classical turbulent motion can be meaningfully formulated in the framework of completely integrable systems. The physical relevance of integrable turbulence theory has been supported by recent fibre optics experiments [7].

Solitons play the key role in the characterisation of nonlinear wave fields in dispersive media, therefore the theory of *soliton gases* in integrable systems comprises an important part of the general theory of integrable turbulence [6]. The very recent observations of dense statistical ensembles of solitons in shallow water wind waves in the ocean [8] well modelled by the KdV equation provide further physical motivation for the development of the theory

of soliton turbulence in integrable systems. In this paper we shall be using the KdV soliton gas as a simplest analytically accessible model yielding a major insight into general properties of soliton gases in integrable systems.

Macroscopic dynamics of a KdV soliton gas are determined by the fundamental ‘microscopic’ properties of two-soliton interactions [9]: (i) soliton collisions are elastic, *i.e.* the interaction does not change the soliton amplitudes (or, more precisely, the discrete spectrum levels in the associated linear spectral problem for the quantum-mechanical Schrödinger operator); (ii) after the interaction, each soliton acquires an additional phase shift; (iii) the total phase shift of a ‘trial’ soliton acquired during a certain time interval can be calculated as a sum of the ‘elementary’ phase shifts in pairwise collisions of this soliton with other solitons during this time interval. These fundamental properties of two-soliton interactions enabled Zakharov in 1971 to introduce the kinetic equation for a rarefied gas of KdV solitons [19]. The generalisation of Zakharov’s equation to finite densities derived in [10] has required the consideration of the thermodynamic-type limit for finite-gap potentials and the associated Whitham modulation equations [11]. A straightforward, physical derivation of the kinetic equation was made in [12]. The effect

of two-soliton collisions on the properties of the statistical moments of nonlinear wave field associated with soliton gas — the soliton turbulence — was studied in [14]. An effective method for the numerical computation of soliton gas was developed in [15] and was applied to the modelling of soliton gases in the KdV and the KdV-BBM (Benjamin–Bona–Mahoni) equations in [16].

The kinetic equation for solitons derived in [10, 12] was shown in [17, 18] to possess some remarkable mathematical properties. In particular, it was shown that it has an infinite number of integrable hydrodynamic reductions which is a strong indication of integrability of the full kinetic equation. Integrability of hydrodynamic reductions opens a broad perspective for obtaining various exact solutions to the kinetic equation. However, the quantitative confirmation of the relevance of the predictions of the soliton kinetic theory to the actual macroscopic dynamics of soliton gases still remains an open problem. Indeed, as was already mentioned, the formal derivation of the kinetic equation for solitons involves certain singular limiting transition of the thermodynamic type. The mathematical conditions required for this transition are not necessarily applicable to physically (or even numerically) accessible soliton systems. This is why it is vitally important to have a direct numerical confirmation of the validity of the kinetic equation. The main goal of the present paper is thus to test the relevance of the soliton gas kinetics to the unapproximated ‘particle dynamics’ of incoherent soliton ensembles. With this aim in view we compare some model exact solutions of the kinetic equation with the results of the high accuracy direct numerical simulations of the KdV soliton gas.

Kinetic equation for a soliton gas. — We consider the KdV equation in the canonical form

$$u_t + 6uu_x + u_{xxx} = 0. \quad (1)$$

We introduce soliton gas as an infinite collection of KdV solitons randomly distributed on the line with non-zero density. This intuitive definition lacks precision but it is sufficient for the purposes of this paper. A mathematically consistent definition of a soliton gas involves the thermodynamic limit of finite-gap potentials (see [13] for details).

Let each soliton in the gas be ‘labelled’ by the spectral parameter $\eta_i \geq 0$ so that $\lambda_i = -\eta_i^2$ is the corresponding discrete eigenvalue in the spectral problem for the linear Schrödinger operator associated with (1) in the inverse scattering transform (IST) formalism. We assume that the discrete values η_i are distributed with certain density on some finite interval, say $[0, 1]$, and replace η_i by the continuous variable $\eta \in [0, 1]$ (see the details in [10, 13, 17]). As is well known (see *e.g.* [9]) the amplitude of an *isolated* KdV soliton with the spectral parameter η is $a = 2\eta^2$ and its speed is $S = 4\eta^2$. It is clear that in the soliton gas, the mean speed of the soliton with the same parameter η will differ from $4\eta^2$. Indeed, due to the pairwise collisions with other solitons (each leading to a ‘phase-shift’)

the distance covered by this ‘trial’ soliton over some time interval $\Delta t \gg 1$ will be different from $4\eta^2 \Delta t$. This intuitive reasoning was used in the original Zakharov paper [19] for the derivation of the *approximate* kinetic equation describing macroscopic dynamics of a rarefied soliton gas.

The full, non-perturbative equation for a ‘dense’ gas of KdV solitons was derived in [10] by considering a singular, thermodynamic type limiting transition for the modulation Whitham equations describing slow evolution of the multiphase solutions of the KdV equation [11]. The result of this limiting transition is the integro-differential kinetic equation [10, 12]

$$f_t + (sf)_x = 0, \quad (2)$$

$$s(\eta) = 4\eta^2 + \frac{1}{\eta} \int_0^1 \ln \left| \frac{\eta + \mu}{\eta - \mu} \right| f(\mu) [s(\eta) - s(\mu)] d\mu \quad (3)$$

for the spectral distribution function $f(\eta) \equiv f(\eta; x, t)$ so that $f(\eta_0; x, t) d\eta dx$ is the number of solitons with the spectral parameter $\eta \in (\eta_0, \eta_0 + d\eta)$ and located in the spatial interval $(x, x + dx)$ at the moment t . The quantity $s(\eta) \equiv s(\eta; x, t)$ is the soliton gas velocity (or the velocity of a “trial” soliton with the spectral parameter η placed in the soliton gas characterised by the distribution function $f(\mu)$). It is important to stress that the typical scales of variations of x and t in the kinetic equation (2) are much larger than in the KdV equation (1), governing the ‘microscopic’ dynamics with $\Delta x, \Delta t = \mathcal{O}(1)$.

The integral

$$\kappa(x, t) = \int_0^1 f(\eta, x, t) d\eta \quad (4)$$

is the total physical (as opposed to spectral) density of the soliton gas, *i.e.* the number of solitons per unit length. Zakharov’s approximate kinetic equation for a rarefied soliton gas [19] is obtained from (2), (3) by assuming $\kappa \ll 1$ and retaining only the first order correction in (3).

In the kinetic description (2), (3) of a soliton gas the solitons are viewed as particles moving with certain speeds and interacting with each other according to the nonlocal closure equation (3). On the other hand, one is also interested in the nonlinear wave field $u(x, t)$ of integrable turbulence associated with the soliton gas dynamics. As is well known (see *e.g.* [4]) a turbulent wave field is usually characterised by the moments $\langle u^n \rangle$ over the statistical ensemble, which, due to ergodicity of soliton turbulence [13], can be computed as spatial averages $\overline{u^n} = \frac{1}{\Delta} \int_0^\Delta u^n(\tilde{x}, t) d\tilde{x}$, over a sufficiently large interval $1 \ll \Delta \ll L$, where L is the typical scale for x -variations in (2).

It was shown in [10, 13, 20] that the two first moments in the KdV soliton turbulence are calculated in terms of the spectral distribution function $f(\eta; x, t)$ as

$$\begin{aligned} \overline{u}(x, t) &= 4 \int_0^1 \eta f(\eta; x, t) d\eta, \\ \overline{u^2}(x, t) &= \frac{16}{3} \int_0^1 \eta^3 f(\eta; x, t) d\eta. \end{aligned} \quad (5)$$

The fundamental restriction imposed on the distribution function $f(\eta)$ follows from non-negativity of the variance

$$\mathcal{A}^2 = \overline{u^2} - \bar{u}^2 \geq 0. \quad (6)$$

The consequences of this restriction have been explored in [20]. Here it will inform the choice of the soliton gas parameters for the numerical modelling.

Hydrodynamic reductions and exact solutions. –

To get a better insight into the properties of the soliton gas dynamics we consider the hydrodynamic reductions of the kinetic equation (2), (3). Such hydrodynamic reductions enable one to derive some simple, physically relevant exact solutions which could then be compared with the results of direct numerical modelling of the KdV equation.

The family of the simplest N -component ‘cold gas’ reductions is selected by the multiflow delta-function ansatz [12]

$$f(\eta; x, t) = \sum_{i=1}^N f_i(x, t) \delta(\eta - \eta_i). \quad (7)$$

Physically, the i -th component of the soliton gas described by the distribution (7) consists of an infinite sequence of nearly identical solitons having the spectral parameter η distributed in a narrow ε -vicinity of $\eta = \eta_i$ such that $\varepsilon/\eta_i \ll 1$, and distributed by Poisson on $x \in (-\infty, \infty)$ with the density $f_i(x, t)$ which can slowly vary in space in time [18], [20]. The hydrodynamic reductions obtained by (7) for arbitrary N have been thoroughly analysed in [17, 18]. Here we shall be mostly looking at the case of a two-component gas yielding the simplest nontrivial results that can be verified numerically. We consider two model problems: (i) the propagation of a ‘trial’ soliton through a one-component ‘cold’ soliton gas and (ii) collision of two one-component soliton gases — the shock tube problem.

Propagation of a trial soliton through one-component soliton gas. We consider a ‘trial’ soliton with the spectral parameter $\eta = \eta_1$ moving through a one-component soliton gas with the distribution function

$$f(\eta; x, t) = f_0(x, t) \delta(\eta - \eta_0), \quad (8)$$

where the density $f_0(x, t)$ is found by the substitution of the distribution (8) into Eqs. (2), (3), yielding the linear transport equation $\partial_t f_0 + 4\eta_0^2 \partial_x f_0 = 0$, describing a trivial translation of the initial distribution function with the constant speed $s(\eta_0) = 4\eta_0^2$, i.e. $f_0(x, t) = F(x - 4\eta_0^2 t)$, where $F(x) \equiv f_0(x, 0)$ is the initial distribution. Substituting the distribution function (8) into the expressions (5) for the moments we obtain from (6) the restriction $f_0 \leq \eta_0/3$ for the soliton gas density [20].

The mean velocity of the trial soliton $s(\eta_1; x, t)$ can then be found from formula (3),

$$s_1(x, t) = 4\eta_1^2 + \frac{1}{\eta_1} \ln \left| \frac{\eta_1 + \eta_0}{\eta_1 - \eta_0} \right| f_0(x, t) [s_1(x, t) - 4\eta_0^2], \quad (9)$$

where $s_1(x, t) \equiv s(\eta_1; x, t)$. Expressing s_1 from (9) we obtain

$$s_1 = 4\frac{\eta_1^2 - \alpha\eta_0^2 f_0(x, t)}{1 - \alpha f_0(x, t)}, \quad \alpha f_0(x, t) \neq 1. \quad (10)$$

Here

$$\alpha = \frac{1}{\eta_1} \ln \left| \frac{\eta_1 + \eta_0}{\eta_1 - \eta_0} \right| > 0 \quad (11)$$

is the classical expression for a phase-shift in a two-soliton collision [9].

Soliton gas shock tube problem. We now consider a two-component soliton gas by introducing the distribution function in the form

$$f(\eta; x, t) = f_1(x, t) \delta(\eta - \eta_1) + f_2(x, t) \delta(\eta - \eta_2), \quad (12)$$

where

$$\eta_{1,2} > 0, \quad \eta_1 \neq \eta_2, \quad f_{1,2} \geq 0. \quad (13)$$

Substitution of (12) into (2), (3) leads to the system of two conservation laws

$$\partial_t f_1 + \partial_x (f_1 s_1) = 0, \quad \partial_t f_2 + \partial_x (f_2 s_2) = 0, \quad (14)$$

$$s_1 = 4\eta_1^2 + \alpha_1(s_1 - s_2)f_2, \quad s_2 = 4\eta_2^2 + \alpha_2(s_2 - s_1)f_1, \quad (15)$$

where $s_{1,2} \equiv s(\eta_{1,2}; x, t)$, and

$$\alpha_{1,2} = \frac{1}{\eta_{1,2}} \log \left| \frac{\eta_1 + \eta_2}{\eta_1 - \eta_2} \right| > 0. \quad (16)$$

It follows from (13), (15) and (16) that if $s_1 > 4\eta_1^2$ then $s_1 > s_2$ and $s_2 < 4\eta_2^2$. Similarly, if $s_1 < 4\eta_1^2$ then $s_1 < s_2$ and $s_2 > 4\eta_2^2$.

We note that, in the degenerate case $\eta_1 = \eta_2 \equiv \eta_0$ the ansatz (12) reduces to the one-component distribution (8) with $f_0 = f_1 + f_2$ as expected. Expressing $s_{1,2}$ in terms of $f_{1,2}$ from (15) we obtain

$$s_1 = 4\eta_1^2 + \frac{4(\eta_1^2 - \eta_2^2)\alpha_2 f_2}{1 - \alpha_1 f_1 - \alpha_2 f_2}, \quad s_2 = 4\eta_2^2 - \frac{4(\eta_1^2 - \eta_2^2)\alpha_1 f_1}{1 - \alpha_1 f_1 - \alpha_2 f_2} \quad (17)$$

provided $f_1 \alpha_1 + f_2 \alpha_2 \neq 1$. Note that by setting $f_1 \equiv 0$ we recover the expression (10) for the speed of the trial soliton s_1 (to establish the correspondence with (10) the index ‘2’ in the first expression (17) should be replaced with 0, also α_2 becomes α). The density of the two-component soliton gas (4) is $\kappa = f_1 + f_2$. It is not difficult to show that Eqs. (14), (15) assume the diagonal form in variables s_1, s_2 [12],

$$\partial_t s_1 + s_2 \partial_x s_1 = 0, \quad \partial_t s_2 + s_1 \partial_x s_2 = 0. \quad (18)$$

System (18) is linearly degenerate which implies (see [17] for the relevant account of the properties of linearly degenerate hydrodynamic type systems): (i) the absence of the nonlinear wave-breaking effects in a two-component soliton gas and (ii) unavailability of simple-wave solutions (indeed one can easily see that the ansatz $s_2(s_1)$ implies that $s_{1,2}$ are constants).

We now consider the Riemann problem for the two-component soliton gas characterised by the spectral distribution function (12) corresponding to the shock tube problem: an initial contact discontinuity separating gases of different density

$$\begin{cases} f_1(x, 0) = f_{10}, & f_2(x, 0) = 0, & x < 0, \\ f_2(x, 0) = f_{20}, & f_1(x, 0) = 0, & x > 0, \end{cases} \quad (19)$$

where $f_{10}, f_{20} > 0$ are some constants satisfying $f_{i0} \leq \eta_i/3$. We also assume that $\eta_1 > \eta_2$. Note that, unlike in the classical gas-dynamics shock tube problem, the initial velocity of the soliton gases is not zero but is fully determined, via Eq. (17), by the density distribution (19).

Since the governing Eqs. (18) are quasilinear the solution of the Riemann problem must depend on x/t alone. Due to linear degeneracy system (18) does not have non-constant simple wave solutions so one has to look for a weak solutions of the original conservation laws (14). The required solution represents a combination of three constant states separated by two contact discontinuities (see [12]). For the total density $\kappa = f_1 + f_2$ we have (see Fig. 3, middle panel, below)

$$\kappa(x, t) = \begin{cases} f_{10}, & x < c^-t, \\ f_{1c} + f_{2c}, & c^-t < x < c^+t, \\ f_{20}, & x > c^+t. \end{cases} \quad (20)$$

The values f_{1c} and f_{2c} of the component densities in the middle region where an interaction of soliton gases occurs, as well as the velocities c^\pm of the contact discontinuities are found from the Rankine–Hugoniot jump conditions,

$$\begin{aligned} -c^-(f_{10} - f_{1c}) + (f_{10}s_{10} - f_{1c}s_{1c}) &= 0, \\ -c^-(0 - f_{2c}) + (0 - f_{2c}s_{2c}) &= 0; \end{aligned} \quad (21)$$

$$\begin{aligned} -c^+(f_{1c} - 0) + (f_{1c}s_{1c} - 0) &= 0, \\ -c^+(f_{2c} - f_{20}) + (f_{2c}s_{2c} - f_{20}s_{20}) &= 0. \end{aligned} \quad (22)$$

Here c^- and c^+ are the velocities of the left and right discontinuity respectively, and f_{1c} , f_{2c} and s_{1c} , s_{2c} are the densities and velocities of the soliton gas components in the interaction region $x \in [c^-t, c^+t]$. The velocities s_{1c} and s_{2c} are expressed in terms of f_{1c} , f_{2c} by relations (17).

Solving (21) and (22) we obtain:

$$f_{1c} = \frac{f_{10}(1 - \alpha_2 f_{20})}{1 - \alpha_1 \alpha_2 f_{10} f_{20}}, \quad f_{2c} = \frac{f_{20}(1 - \alpha_1 f_{10})}{1 - \alpha_1 \alpha_2 f_{10} f_{20}}. \quad (23)$$

The speeds c^\pm of the boundaries of the interaction region are given by

$$\begin{aligned} c^- &= 4\eta_2^2 - \frac{4(\eta_1^2 - \eta_2^2)\eta_1 f_{1c}}{1 - \alpha_1 f_{1c} - \alpha_2 f_{2c}}, \\ c^+ &= 4\eta_1^2 + \frac{4(\eta_1^2 - \eta_2^2)\alpha_2 f_{2c}}{1 - \alpha_1 f_{1c} - \alpha_2 f_{2c}}. \end{aligned} \quad (24)$$

The expanding interaction region in the soliton gas shock tube problem can be viewed as a stochastic counterpart of the traditional, coherent dispersive shock wave

(DSW) forming due to a dispersive regularisation of the Riemann initial data in the KdV equation [21] (we need to make a clear distinction between the studied here incoherent DSWs occurring in physical space, and the incoherent DSWs recently observed in the Fourier spectra evolution of random waves [22]). In contrast with the coherent DSWs, the incoherent DSW generated in the collision of two soliton gases does not have a distinctive structure of a slowly modulated wavetrain but is characterised by the uniformly increased intensity of fluctuations \mathcal{A}^2 (6) compared to the values of \mathcal{A}^2 in the colliding soliton gases at $t = 0$. It is not difficult to show that the density of the two-component soliton gas in the incoherent DSW region, $\kappa_c = f_{1c} + f_{2c} > f_{10}, f_{20}$ but $\kappa_c < f_{10} + f_{20}$.

Numerical experiments. – In this section we perform direct numerical simulations of the KdV soliton gas and compare the numerical solutions with the corresponding exact solutions of the kinetic equation obtained in the previous section.

In order to solve numerically the KdV equation we employ the standard pseudo-spectral Fourier collocation technique [23, 24]. This method is briefly explained below. Denote by $\hat{u}(k, t) = \mathcal{F}\{u\}$ the Fourier transform of $u(x, t)$ in x , where k is the wavenumber. Then, by Fourier-transforming Eq. (1) yields $\hat{u}_t - ik^3 \hat{u} = -3ik(\hat{u}^2)$. The most computationally efficient way consists in computing the spatial derivatives in spectral space while the nonlinear product is computed in real space and dealised using the classical 3/2th rule. In order to improve the time-stepping we will use the so-called integrating factor technique. This consists of the exact integration of the linear terms [24]. This allows to increase substantially the accuracy and the stability region of the time marching scheme [23]. Finally, the resulting system is discretized in time by the Verner's embedded adaptive 9(8) Runge–Kutta scheme [25]. The time step is adapted automatically according to the H211b digital filter approach [26].

Test 1: Propagation of a trial soliton through a one-component gas. We now present the results of the numerical simulation of the propagation of a trial soliton with given spectral parameter $\eta = \eta_1$ through the one-component soliton gas with $\eta = \eta_0$ to compare with the theoretical results. The value for the comparison is the mean (*i.e.* averaged over a large interval) velocity of the trial soliton given by formula (10) in which $f_0 = \text{const}$.

In the simulations, the initial condition for the one-component KdV soliton gas is composed of finite but sufficiently large number M of solitons (in our experiments $M = 200$) with the random amplitude $a = 2\eta^2$ chosen from the normal distribution of the spectrum η with mean η_0 and fixed standard deviation $\sigma = 2 \times 10^{-2}$, separated by a space lag Δ_0 whose value is directly related to the gas density:

$$w(x, 0) = \sum_{i=1}^M 2\eta_i^2 \text{sech}^2(\eta_i[x - (\ell + i\Delta_0 + \epsilon_i)]). \quad (25)$$

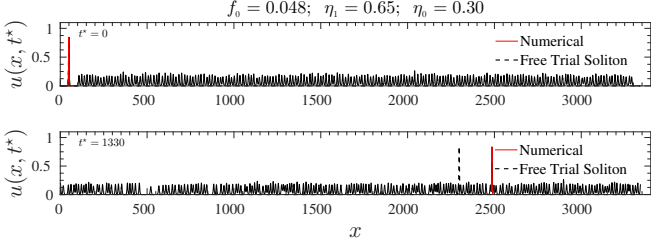


Fig. 1: Comparison for the propagation of a free soliton with $\eta_1 = 0.65$ in a void (black dashed line) with the propagation of the trial soliton with the same spectral parameter (red solid line) through a soliton gas with the dominant spectral component $\eta_0 = 0.3$ and density $f_0 = 0.048$. One can see that the trial soliton gets accelerated due to the interactions with smaller solitons in the gas.

The parameters ℓ and ϵ_i are respectively the starting point of the random lattice and a random (uniform) perturbation to the i -th soliton position, taken in the interval $\epsilon_i \in (-1, 1)$. So that, in order to increase (or decrease) the density κ_0 , it is only required to change the value of Δ_0 .

With an added trial η_1 -soliton the initial-boundary conditions for the KdV equation (1) assume the form

$$\begin{aligned} u(x, 0) &= 2\eta_1^2 \text{sech}^2(\eta_1 x) + w(x, 0), \\ u(x + 2L, t) &= u(x, t). \end{aligned} \quad (26)$$

The snapshots of the trial soliton evolution are shown in Fig. 1. One can see that the trial soliton undergoes a noticeable acceleration as predicted by the theory. The quantitative comparisons of the numerically found values for the averaged speed of the trial soliton with the formula (9) are shown in Fig. 2(a, b) for two different sets of parameters of the soliton gas. The comparisons in Fig. 2(a, b) show excellent agreement between the results of direct numerical simulations and the predictions of the kinetic theory. In all simulations the condition (6) restricting the soliton gas density (see [20]) is satisfied.

Test 2: Soliton gas shock tube problem. Following the strategy proposed in the previous section, we build the initial condition as a superposition of two distinct populations of solitons separated at $t = 0$ by an empty gap, so that $u(x, 0) = w_1(x, 0) + w_2(x, 0)$. As in the previous case the amplitudes $2\eta^2$ of the two gas components ($w_1(x, 0)$ and $w_2(x, 0)$) are specified by the Gaussian random values distributed with the means η_1 and η_2 and standard deviations $\sigma_1 = 10^{-4}$ and $\sigma_2 = 2 \times 10^{-2}$ respectively. Again, the respective densities f_{10} and f_{20} can be easily changed by tuning the parameters Δ_1 and Δ_2 . The numerical solution of the KdV equation with this initial condition is presented in Fig. 3. We now perform the comparison of the parameters of this numerical solution with the weak analytical solution (20) of the soliton gas shock tube problem. Specifically, we are interested in comparing the total density of solitons $\kappa_c = f_{1c} + f_{2c}$ in the interaction (in-

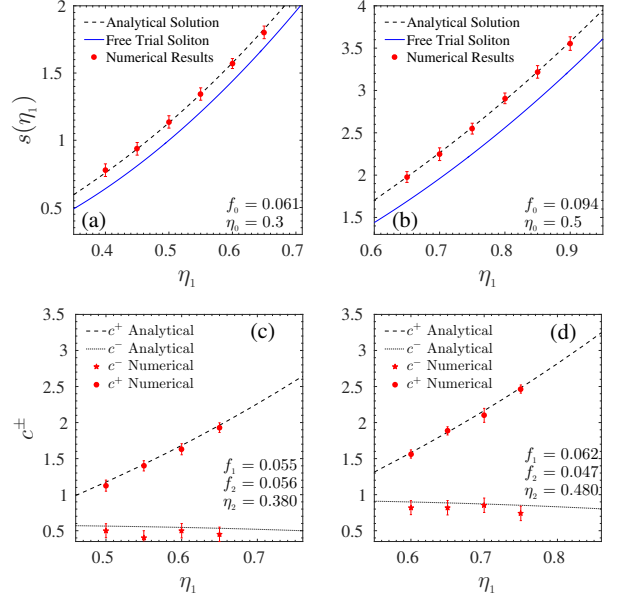


Fig. 2: Comparison of the kinetic theory prediction (9) for the average speed of a large trial soliton propagating through a one-component soliton gas with the results of direct numerical simulations of the KdV soliton gas) panels (a, b); panels (c, d): Comparisons for the shock tube problem: the speeds c^\pm of the edges of the interaction region.

coherent DSW) region and in the speeds c^\pm of its edges.

The comparisons for the velocities of the edges of the interaction region (incoherent DSW) is presented in Fig. 2 (c, d) and demonstrate excellent agreement between the analytical and numerical results.

The comparisons for the total density as the function of time in the interaction region is presented in Fig. 4(a, b). One can see three distinct regions in these plots. The value of the total density is initially equal to the sum $f_{10} + f_{20}$ of the component densities and then decreases through the equilibration process to the stationary value κ_c (highlighted in all three plots) which is in excellent agreement with the predictions of the theory based on the weak solution (20). The subsequent decrease of the density seen in the numerical plots is due to an inherent restriction of the numerical experiment involving finite number of solitons so the interaction region is sustained only for a finite interval of time.

We shall now compare the values of the two first moments (5), which for the interaction region assume the form, on using the ansatz (12),

$$(\bar{u})_c = 4(\eta_1 f_{1c} + \eta_2 f_{2c}); \quad (\bar{u}^2)_c = \frac{16}{3}(\eta_1^3 f_{1c} + \eta_2^3 f_{2c}),$$

where f_{1c} and f_{2c} are determined in terms of the initial data by formulae (23). The results of the comparison are presented in Fig. 4(d). Again, the excellent agreement is observed. One can also see that the condition (6), $\mathcal{A}_c^2 = (\bar{u}^2)_c - (\bar{u})_c^2 \geq 0$, is satisfied.

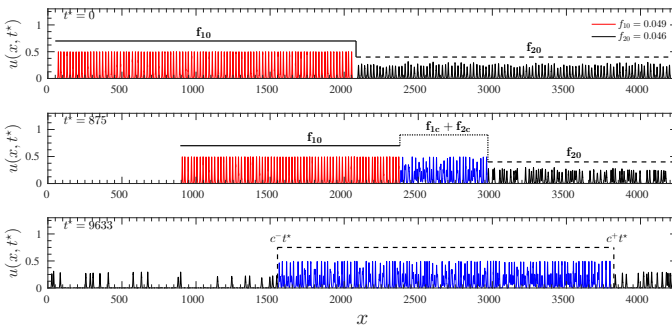


Fig. 3: *Soliton gas shock tube problem: numerical solution of the KdV equation. The expanding incoherent DSW region due to the interaction of two cold soliton gases is shown in blue.*

Conclusions. — We have undertaken a detailed comparison of the macroscopic dynamics of the KdV soliton gas predicted by the kinetic equation for solitons with the results of direct numerical simulations of the KdV equation. The simulations involved 200 solitons enabling an accurate determination of macroscopic parameters of the soliton gas. Two test problems have been considered: the propagation of a trial soliton through a one-component ‘cold’ soliton gas and the shock tube problem involving the interaction of two cold gases with different parameters leading to the formation of an incoherent dispersive shock wave. In both cases an excellent agreement between the asymptotic analytical predictions of the kinetic equation and the direct KdV ‘molecular dynamics’ numerical simulations has been observed. This confirms validity of the kinetic equation for solitons as a quantitatively accurate model for the description of non-equilibrium dynamics of soliton gases in integrable systems. The challenging problem is now to study the structure and evolution of the definitive statistical characteristics of integrable soliton turbulence (PDF, power spectrum density etc.). This will be the subject of future work.

Acknowledgement. — GE is grateful to A. Kamchatnov for numerous stimulating discussions.

REFERENCES

- [1] A. R. Osborne, *Nonlinear ocean waves and the inverse scattering transform*, Amsterdam, Elsevier (2010).
- [2] J. Lauriea et al. *Physics Reports* **514** (2012) 121–175.
- [3] A. Picozzi et al., *Physics Reports*, **542** (2014) 1–132.
- [4] S. Nazarenko, *Wave turbulence*, Springer (2011).
- [5] C. Kharif, E. Pelinovsky and A. Slunyaev, *Rogue waves in the ocean*, vol. 14. *Advances in Geophysical and Environmental Mechanics and Mathematics*. Berlin, Germany: Springer (2009).
- [6] V.E. Zakharov, *Stud. Appl. Math.* **122** (2009) 219–234.
- [7] S. Randoux et al., *Phys. Rev. Lett.* **113** (2014) 113902.
- [8] A. Costa et al., *Phys. Rev. Lett.* **113** (2014) 108501.
- [9] P.G. Drazin and R.S. Johnson *Solitons: an introduction*. Cambridge University Press (1993).
- [10] G.A. El, *Phys. Lett. A* **311** (2003) 374–383.

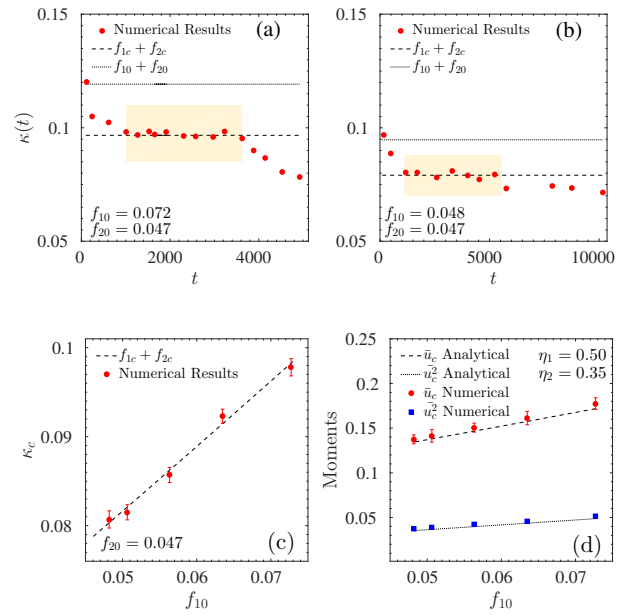


Fig. 4: *Soliton gas shock tube problem: total density in the interaction region as a function of time (a, b). The highlighted regions correspond to the equilibrium state; (c) the equilibrium total density $\kappa_c = f_{1c} + f_{2c}$ in the interaction region as a function of the density f_{10} of the ‘left’ gas. The density of the ‘right’ gas $f_{20} = 0.047$; (d) the moments of the random wave field in the interaction region.*

- [11] G.B. Whitham, *Linear and Nonlinear Waves* (Wiley–Interscience, New York, 1974).
- [12] G.A. El and A.M. Kamchatnov, *Phys. Rev. Lett.* **95** (2005) 204101.
- [13] G.A. El et al., *Physica D* **152–153** (2001) 653–664.
- [14] E.N. Pelinovsky et al., *Phys. Lett. A* **377**, (2013) 272.
- [15] D. Dutykh, M. Chhay, and F. Fedele, *Comp. Math. Math. Phys.*, **53** (2013) 221–236.
- [16] D. Dutykh and E. Pelinovsky, *Phys. Lett. A* **378** (2014) 3102–3110.
- [17] G.A. El et al., *J Nonlin. Sci.* **21** (2011) 151–191.
- [18] M.V. Pavlov, V.B. Taranov and G.A. El, *Theor. Math. Phys.* **171** (2012) 675–682.
- [19] V.E. Zakharov, *JETP*, **33** (1971) 538–541.
- [20] G.A. El, *Chaos* **26** (2) (2016), arXiv:1512.02470.
- [21] A.V. Gurevich and L.P. Pitaevskii, *Sov. Phys. JETP* **38** (1974) 291–297.
- [22] J. Garnier et al., *Phys Rev. Lett.* **111** (2013) 113902.
- [23] L.N. Trefethen, *Spectral methods in MatLab*, (L. N. Trefethen, Ed.), SIAM, Philadelphia, PA, USA (2000).
- [24] J.P. Boyd, *Chebyshev and Fourier Spectral Methods*, Dover Publications New York, (2nd ed.) (2000).
- [25] J.H. Verner, *SIAM J. Num. Anal.*, **15** (1978) 772–790.
- [26] G. Soderlind, *ACM Trans. Math. Software*, **29** (2003) 1–26.